Organic modification of montmorillonite and effect of catalytic selectivity on thedimerization of unsaturated fatty acid

XUE HUANG

GUOQIANG YIN

GUANGZHU FENG

Organic modification of montmorillonite and effect of catalytic selectivity on the dimerization of unsaturated fatty acid

Xue HUANG, Guoqiang YIN, Guangzhu FENG[*]
College of Chemistry and Chemical Engineering, Zhongkai University of Agriculture and Engineering, Guangzhou,
Guangdong, P.R. China

Abstract: This study describes the selective synthesis of C_{36}-dimer fatty acids, by reacting unsaturated fatty acid at 533 K for 6 h in the presence of montmorillonite and lithium chloride as the catalyst and cocatalyst, respectively. The catalytic performance of different montmorillonite and organic modified montmorillonite catalysts was investigated in the dimerization of technical grade unsaturated fatty acid, and the influence of the catalyst structure and composition on the catalytic performance was analyzed. All the samples were characterized by X-ray diffraction (XRD), Fourier transform-infrared spectroscopy (FT-IR), scanning electron microscope (SEM), transmission electron microscopy (TEM), thermogravimetry (TG), and dispersion experiments. The results show that the layer spacing and dispersion property of the montmorillonite crystal have important effects on its catalytic performance and the yield of the product. In the dimerization experiments, the maximum yield of the dimer acid is found to be 70.15%, while the lowest yield is 32.37%. It is thought that the larger interlayer spacing in the montmorillonite provides more reaction space for the unsaturated fatty acid, allows the generation of a large volume of dimeric molecules, and helps the product molecules to diffuse out from the layered structure.

Key words: Montmorillonite, modification, dimerization, dimer acid

1. Introduction

Dimer acids are generally dimeric polymers synthesized by two identical or different unsaturated fatty acids having 18-carbon atoms, such as tall oil, oleic acid, linoleic acid, soybean oil, cottonseed oil, sunflower oil, rapeseed oil, and other unsaturated aliphatic fatty acids.[1] Dimer acids are very useful chemical intermediates due to their wide range of starting materials, chemical reactivity, and good performance stability, as well as their structural characteristics. Dimer acids and their derivatives can be used to prepare polyamide resins, paints, lubricants, fuel oil additives, corrosion inhibitors, and other important fine chemical products.[2−4] Since the 1950s, several commercially available dimer acids have been synthesized by the catalytic synthesis of clay at 503∼523 K. Since the 1970s,[5−7] the industrial production of dimer acids has shown a steady increase. However, the current methods of synthesis of dimer acids have several drawbacks, such as the deep color of the products, low yields, and decarboxylation side reactions accompanied by high temperature. Thus, better alternative production methods are being explored.

There are two kinds of catalysts used in the synthesis of dimer acids: homogeneous catalysts and heterogeneous catalysts. The traditional catalysts used for the polymerization of dimer acids are homogeneous

---

[*]Correspondence: fengguangzhu@163.com

catalysts, such as alkali or alkaline metal salts[8] and Lewis acids.[9,10] Compared to the homogeneous catalysts, heterogeneous catalysts are more environmentally friendly, widely available, inexpensive, easy to separate from the products and reuse, and commercially more attractive. Heterogeneous catalysts are mainly clays and clay materials,[11−15] such as kaolin, montmorillonite (MMT), sepiolite, and bentonite.

Cation-exchange modified montmorillonite is widely used in the dimerization of fatty acids,[11,14] because MMT is a natural raw material, abundant in nature, easy to use, and has excellent physicochemical properties.[16−18] Addition of a cocatalyst, such as LiOH, LiCl, $Ca(OH)_2$, and Na_2CO_3, can increase the yield of the dimer acids. Since the lithium ion has a small radius, large charge density, and strong polarity, it has a higher tendency to covalently bond with chloride ions. The bond has more significant covalency than the chemical bond of other alkali chlorides. Moreover, because the valence bond of lithium chloride is not a typical ionic bond, it can be dissolved in many organic solvents, showing lipophilic properties. In addition, chloride ion has strong nucleophilic ability, which makes lithium chloride enjoy charge separation characteristics. On the other hand, the hydrophilicity of montmorillonite affects the adsorption and mass transfer of unsaturated fatty acids. The amount, type, and intensity of interlayer catalytic sites all affect the catalytic properties of montmorillonite. Overall, the lipophilicity of montmorillonite can be improved by the lipophilic properties of LiCl, and the catalytic performance of montmorillonite enhanced by the presence of lithium ions. The highest yield of dimer acids from the polymerization of tall oil was about 71% by using 6 *wt.*% MMT at 503 K.[15] Tall oil was dimerized over a clay containing LiOH, and 65 wt.% of different kinds of dimer acids (linear, alicyclic, aromatic, and polycyclic) were formed.[16] The maximum dimer yield was obtained over modified smectites with magnesium as interlayered cation. However, addition of Na_2CO_3 to montmorillonite strongly decreased the yield of dimerization.[14,19,20]

Mechanistic studies have been performed to understand the dimerization process; however, the complex reaction mechanism for the dimerization of unsaturated fatty acids over the clays is still not very clear. It is widely accepted that a combination of isomerization, conjugation, Diels–Alder cycloaddition, and hydration/dehydration reactions is involved. The obtained product is a mixture of monomers, dimers, and trimers as well as linear, cyclic, and aromatic structures.[21]

The purpose of the present study was to evaluate the dimerization rate of technical grade unsaturated fatty acid (linoleic acid:oleic acid ratio of about 2:1) with organic modified montmorillonite (OMMT) and LiCl, which was modified with different cationic surfactants. The effects of nine different catalysts, interlayer spacing, and dispersion properties of catalysts on the yield of the dimer acid product were evaluated.

2. Results and discussion

2.1. Analysis of OMMT

XRD analysis. According to Bragg's law $n\lambda = 2d\sin\theta$ ($n = 1$, $\lambda = 1.5418$ Å) and the position of 001 diffraction peaks, the corresponding layer spacing can be calculated. The interlayer spacing values of the modified OMMTs were analyzed by XRD. The d-spacing of first-insert OMMT increased gradually with the increase in content of the intercalation agent. When the content of the intercalation agent was 3 CEC of MMT, the d-spacing reached the maximum, because the modifier solution did not provide enough cations. The experiments did not use intercalation agent amounts more than 3 CEC, because the reaction flask was filled with foam at 3 CEC. A large amount of foam will affect the full contact of quaternary ammonium salts with montmorillonite particles.

XRD patterns (Figure 1) were used to observe the differences between pristine MMT and first-insert OMMT. The 001 diffraction peaks for pristine MMT, DTAB-MMT, STAC-MMT, CTAB-MMT, and HTAC-MMT were at $2\theta = 5.97, 4.49, 2.18, 2.33$ and $2.31°$, respectively, corresponding to d-spacing values of 1.48, 1.97, 4.06, 3.80 and 3.82 nm. After the intercalation of the agent, the 001 diffraction peak shifted to the left. The XRD pattern of DTAB-MMT showed only one major broad peak similar to that of Na-MMT. The curves of the other three OMMTs showed two peaks below $6°$, with high intensity peaks at $2\theta = 2\sim3°$. The interlayer space of the first-insert OMMT expanded significantly after modification, which clearly indicated that the intercalation agent had successfully inserted into the interlayer space of Na-MMT. The interlayer space-widening effect of the intercalation agent was in the following order: STAC > HTAC $\approx$ CTAB > DTAB, which is consistent with the carbon chain length of the intercalation agent.

The d-spacing of second-insert OMMT reached the maximum value at 2 CEC of the intercalation agent. When the content of the intercalation agent was 3 CEC of Na-MMT, the d-spacing decreased. XRD patterns of the second-insert OMMT samples are shown in Figure 2.
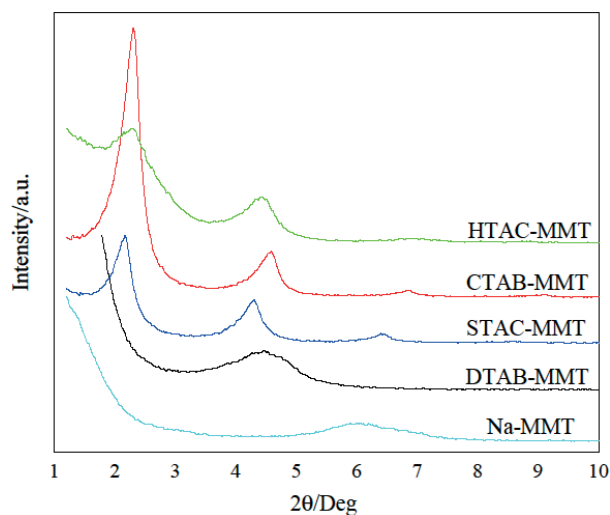

Figure 1. XRD patterns of MMT and first-insert OMMT at 3 CEC of MMT.
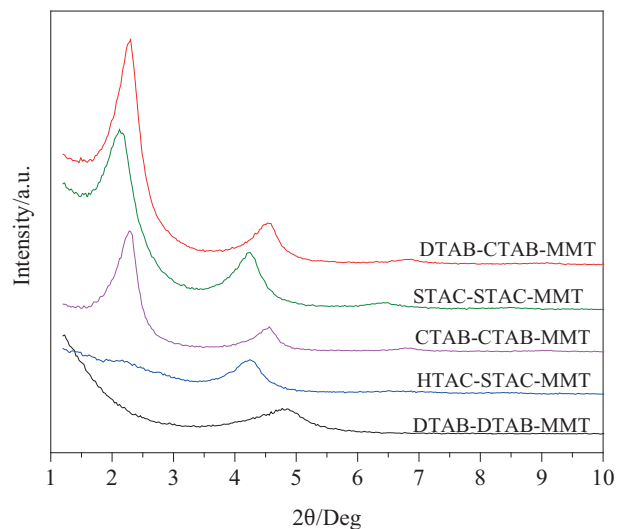

Figure 2. XRD patterns of MMT and second-insert OMMT at 2 CEC of MMT.

As shown in Figure 2, the 001 diffraction peaks for STAC-STAC-MMT and HTAC-STAC-MMT were at $2\theta = 2.19°$ and $2.20°$, corresponding to the widest d-spacing values of 4.03 nm and 4.01 nm, respectively. Compared to the first-insert OMMT, the 001 diffraction peaks of the second-insert OMMT moved to the left were not obvious. After the second-insert, the interlayer spacing of DTAB-DTAB-MMT and STAC-STAC-MMT was not changed. The 001 diffraction peak for HTAC-STAC-MMT was a single broad peak. The other layer spacing showed a substantial increase, clearly indicating the intercalation of the agent into the first-insert interlayer space of OMMT.

Considering the example of CTAB, from the thickness of the MMT layer (9.6 Å)[22] and the stabilized alkyl chain length of the CTAB (4.6 Å, 20.035 Å),[23] it is clear that during the first intercalation, the CTAB molecules form a bilayer in the interlayer region (Figure 3).

During the second intercalation, when more and more of the CTAB molecules are absorbed into the interlayer, they change from the parallel to the tilted bilayer form in the interlayer region. Thus, the second intercalating CTAB molecules form the tilted bilayer in the interlayer of MMT. The observation that the
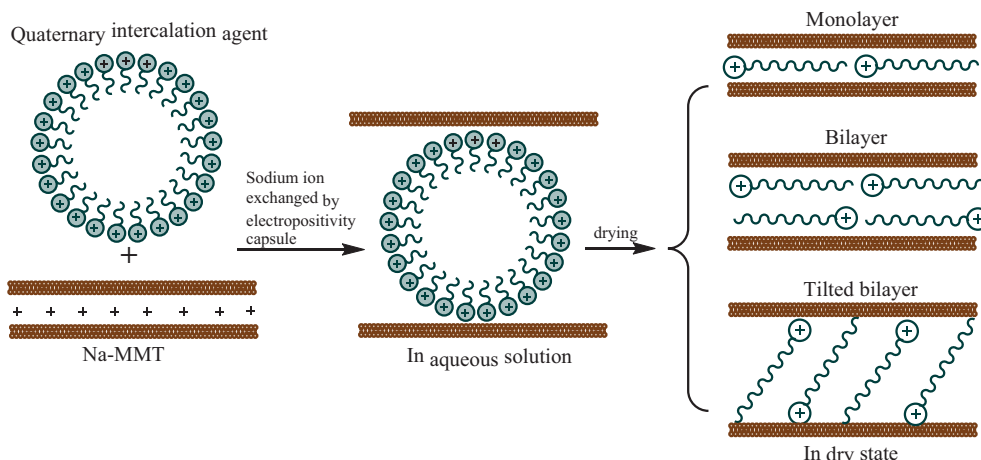
Figure 3. Schematic drawings of Na-MMT in the presence of organic cations.

intensity of the 001 peak at $2\theta = 2.31°$ of CTAB-CTAB-MMT became stronger is in accordance with the TEM results.

SEM analysis. Figure 4 gives SEM micrographs of Na-MMT (Figure 4a), STAC-MMT (Figure 4b), and STAC-STAC-MMT (Figure 4c). The SEM micrographs show that MMT with further modification resulted in more loosened organo-clays, attributed to the expansion of interlayer space after intercalation reactions.
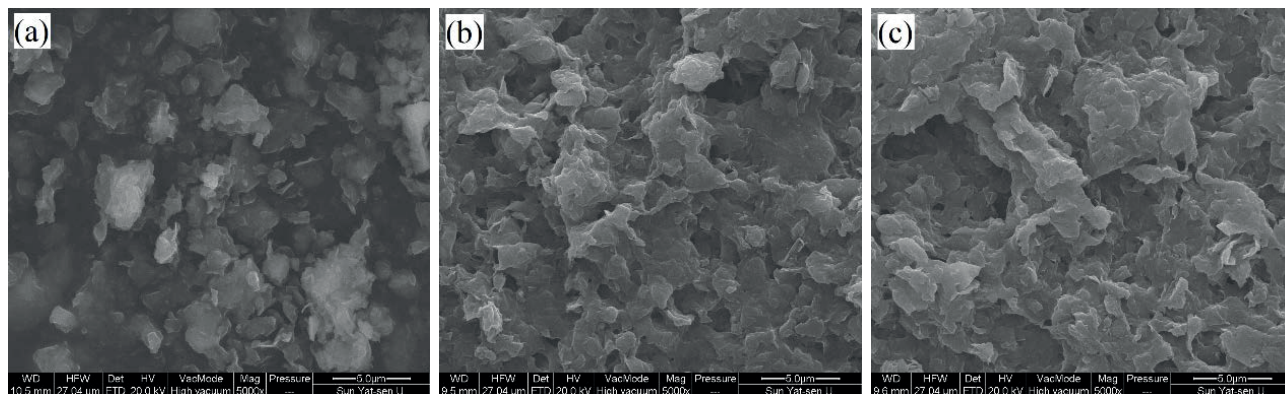

Figure 4. SEM micrographs of (a) Na-MMT, (b) STAC-MMT, and (c) STAC-STAC-MMT.

Figure 5 shows SEM micrographs of single particles of Na-MMT (Figure 5a), STAC-MMT (Figure 5b), and STAC-STAC-MMT (Figure 5c). The Na-MMT was a compact spherical particle. After modification, the surfaces of particles of OMMT became disordered. The compact spheres evolved into expanded and multilayer structures that could be observed on the surfaces of the particles. The structure evolution was mainly due to the change in the interlayer spacing of montmorillonite. Compared to STAC-MMT, the multilayer structure of STAC-STAC-MMT was looser. This was because after the second modification the layer spacing of MMT was further expanded.

TEM analysis. Figure 6 shows the TEM images of Na-MMT (Figure 6a), first-insert OMMT (Figures 6b–6d), and second-insert OMMT (Figures 6e–6h). As seen from Figure 6, after the first-insert, the introduction of the intercalation reagent into the Na-MMT system caused MMT to be aggregated together with a noticeable separation of the clay layer. After the second-insert, the interlayer spacing expanded further and was much
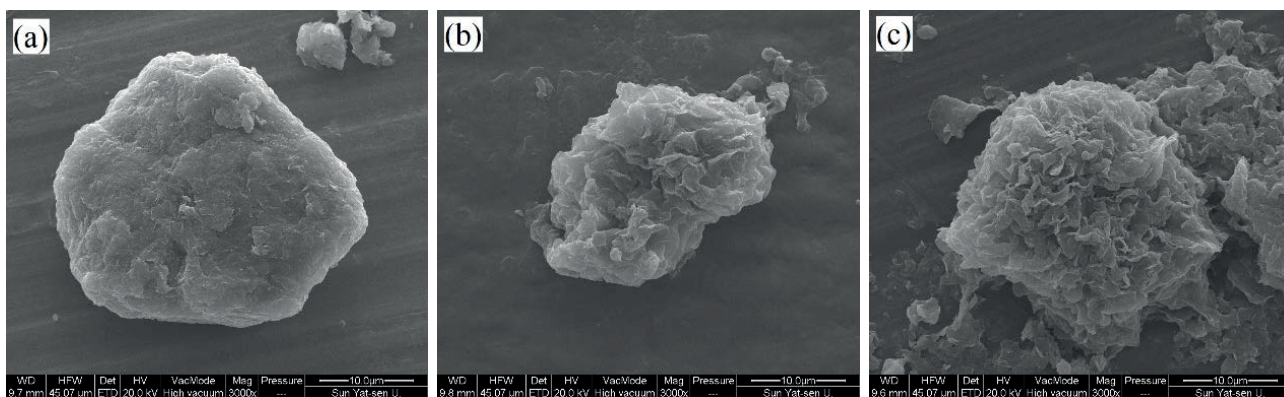
Figure 5. SEM micrographs of single particles of (a) Na-MMT, (b) STAC-MMT, and (c) STAC-STAC-MMT.

larger than that of Na-MMT. It is well known that due to the different physical and chemical properties of organic and inorganic components it is difficult to obtain exfoliated clay directly through the melt mixing method.[24,25] Thus, the cationic surfactant was intercalated successfully into the clay.
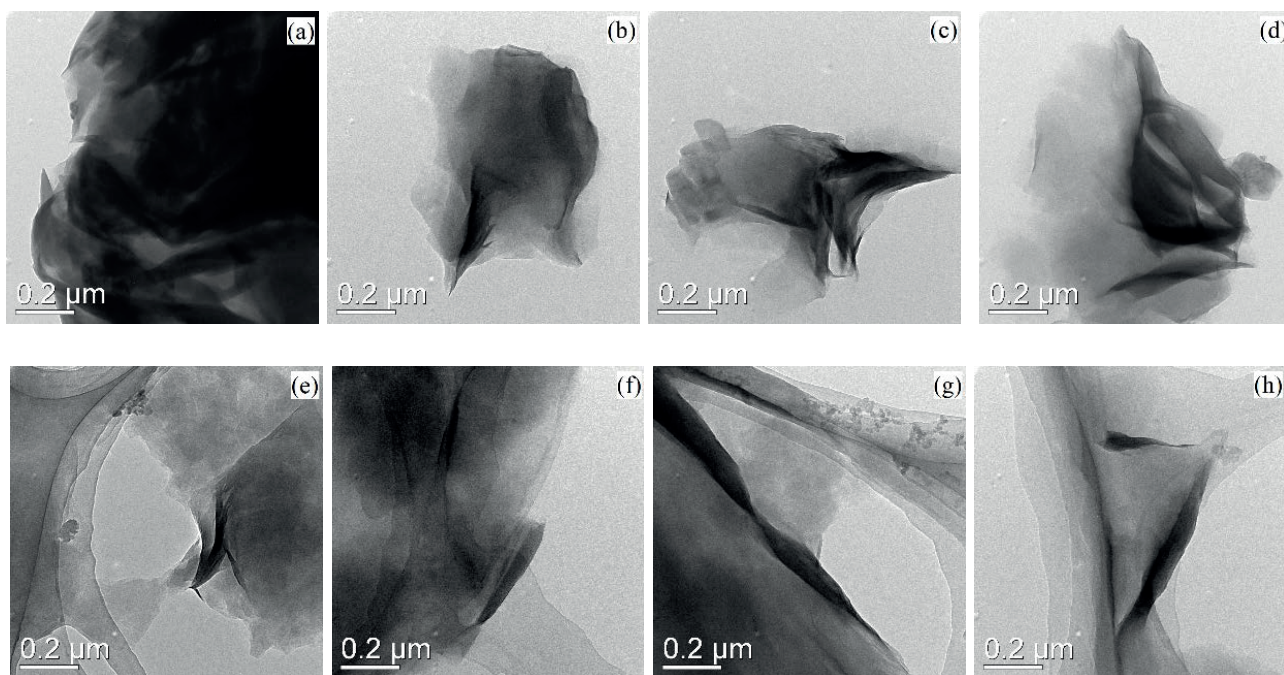

Figure 6. TEM images of (a) Na-MMT; (b), (c), (d) first-insert OMMT of DTAB-MMT, CTAB-MMT, and HTAC-MMT, respectively; (e), (f), (g), (h) second-insert OMMT of CTAB-CTAB-MMT, DTAB-CTAB-MMT, HTAC-STAC-MMT, and STAC-STAC-MMT, respectively.

FT-IR analysis. FT-IR analyses (Figure 7a) provided further structural information on MMT, first-insert OMMT, and second-insert OMMT. The hydroxyl (–OH) stretching vibration of the characteristic structure of Na-MMT appeared at 3620 cm^{-1} as a broad band, while the –OH bending vibration band occurred at 1639 cm^{-1}. Moreover, the Si–O stretching vibration band was observed at 1032 cm^{-1} and the interlayer water stretching vibration appeared at 3450 cm^{-1}. Curves of other samples showed the characteristic peaks of Na-MMT, indicating that the layered structure of MMT was not destroyed after modification.
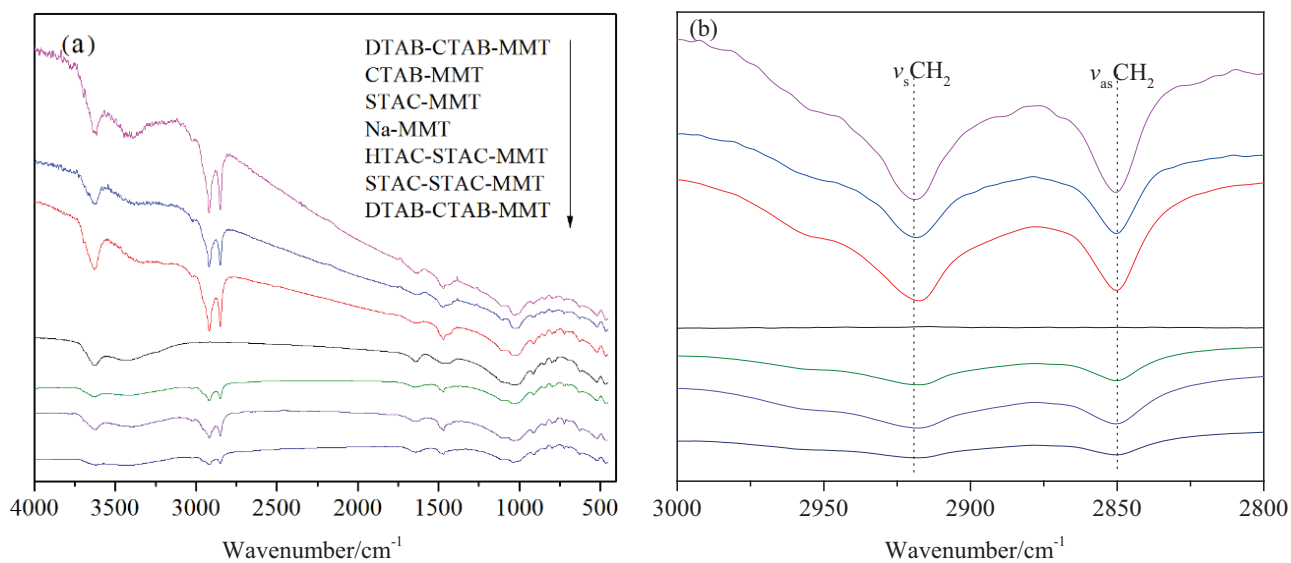
Figure 7. FT-IR spectra of (a) Na-MMT and OMMT; (b) the larger image in the wavenumber range from 3000 to 2800 cm^{-1}.

Compared with the FT-IR spectrum of the Na-MMT, several distinct changes were observed in that of OMMT from 3000 to 2800 cm^{-1}, absorption peaks at 2850 cm^{-1} and 2918 cm^{-1} were created, which were in accordance with the unsymmetrical stretching vibration and symmetrical stretching vibration of –CH$_2$, respectively, and the spectra are shown in Figure 7b. These results indicate that organic macromolecular chains of the intercalation agent penetrated into the silicate interlayer areas of the Na-MMT.

TG analysis. Figure 8 displays the thermal stability of MMT and OMMT determined using thermogravimetric (TG) techniques. The TG curves in Figure 8a provide information on the first-insert OMMT samples. The weight loss of the samples increased with increase in the molecular weight. The TG behavior of second-insert OMMT samples in Figure 8b was also consistent with this trend.
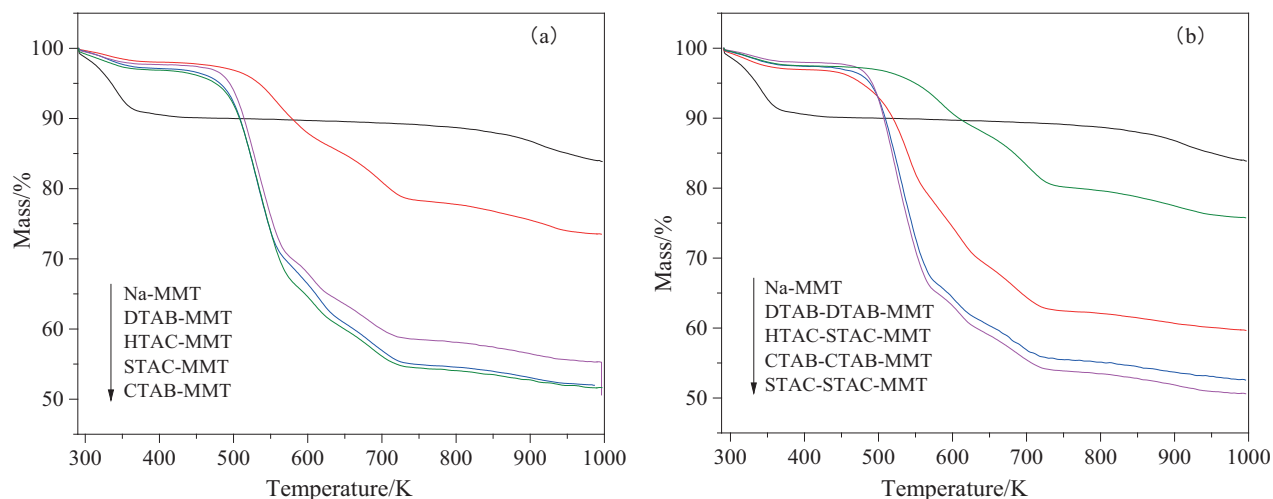

Figure 8. TG thermograms of (a) the first-insert OMMT; (b) the second-insert OMMT.

The water adsorbed on the surface of MMT was mainly lost from 293 to 413 K. The loss rate of MMT was 8.87%, while the loss rates of first-insert OMMT and second-insert OMMT were less than 2.1% (Table 1).

Table 1. The mass loss of samples

Samples	Surface water content/% 293∼413 K	Interlayer water content/% 413∼503 K	Intercalation agent content/% 503∼873 K
Na-MMT	8.87	0.37	2.41
DTAB-MMT	1.81	1.21	20.58
CTAB-MMT	1.84	6.35	39.20
HTAC-MMT	2.03	4.34	36.29
STAC-MMT	2.67	5.60	37.87
DTAB-DTAB-MMT	2.28	0.62	18.65
HTAC-STAC-MMT	2.71	4.21	31.56
DTAB-CTAB-MMT	2.63	4.28	35.55
CTAB-CTAB-MMT	2.28	5.37	37.88
STAC-STAC-MMT	2.67	5.47	38.27

The surface adsorbed water of OMMT was obviously less than that of Na-MMT. This indicates that the surface energy of MMT was decreased due to insertion of the intercalation agent, and the hydrophilic silicate surface was converted to a hydrophobic one.[26] The interlayer water of MMT was eliminated from 473 K to 503 K. There was little water between the MMT layers; thus this step was not obvious at 473∼503 K. The mass loss rate of the interlayer water in the second-insert OMMT was smaller than that in the first-insert OMMT, since the interlayer water of the second-insert OMMT was partially replaced by the secondary intercalation agent. The organic content between the layers decomposed from 503 to 873 K. Both the first-insert and second-insert OMMT showed mass loss in this range, indicating that the organic matter had been effectively intercalated. After 873 K, a part of the M–OH bond in the montmorillonite structure broke and the structural water began to be eliminated. Based on the XRD and TG results, it can be concluded that the inorganic cations in MMT were replaced by the intercalation agent, and that the intercalation agent molecules had inserted into the layers of clay successfully.

Dispersibility analysis. The purpose of montmorillonite modification was to improve the compatibility and dispersibility of OMMT in unsaturated fatty acid. In order to investigate the dispersion ability and optimize the parameters for improved polymerization of unsaturated fatty acid, water and unsaturated fatty acid were selected as the dispersion media to evaluate the compatibility of OMMT. The experimental results are shown in Table 2.

Table 2. Dispersibility of Na-MMT and OMMT in deionized water and unsaturated fatty acid (with CTAB as example).

Dispersion medium	Na-MMT	CTAB-MMT	CTAB-CTAB-MMT
deionized water	++(cloudy)	—	— —
unsaturated fatty acid	——	+	++

++ : better dispersibility, supernatant is uniform; +: good dispersibility; —: bad dispersibility; ——worse dispersibility, the sample at the bottom of the bottle

Table 2 shows that the lamellar surface lipophilicity of first-insert OMMT was improved, but its compatibility with unsaturated fatty acid was not very good. On the other hand, the dispersibility of second-insert OMMT in unsaturated fatty acid was further improved. It can be seen that the secondary intercalation agent in-

troduced in the interlayer improved the properties of the OMMT further compared to the primary intercalation modification.

2.2. Dimerization analysis

Catalytic synthesis of dimer acids by Na-MMT. Addition of cocatalysts can improve the yield of dimer acids. Thus, unsaturated fatty acid dimerization experiments were performed with Na-MMT as catalyst and LiCl as cocatalyst. The effects of various factors (such as reaction temperature, reaction time, and dosages of catalyst and cocatalyst) on the yield of dimer acid were studied by orthogonal experiments under atmospheric pressure. The different reaction conditions and results of the orthogonal experiments are shown in Table 3.

Table 3. The factors and results of orthogonal experiment.

No.	Temperature/K A	Reaction time/h B	w(Na-MMT)/% C	w(LiCl)/% D	Yield/%
1	513	4	10	1.0	19.50
2	513	6	12	1.2	30.11
3	513	8	14	1.4	25.46
4	533	4	12	1.4	31.28
5	533	6	14	1.0	28.80
6	533	8	10	1.2	29.52
7	553	4	14	1.2	22.66
8	553	6	10	1.4	24.31
9	553	8	12	1.0	23.43
k_1	25.023	24.480	24.433	23.910	
k_2	29.867	27.740	28.273	27.430	
k_3	23.467	26.137	25.640	27.017	
R	6.400	3.260	3.830	3.520	
Order of factor influence		A > C > D > B			
Appropriate level		A_2 C_2 D_2 B_2			

As seen from Table 3, the effects of the different factors on the dimer acid yield followed the order: reaction temperature > dosage of Na-MMT > reaction time > dosage of LiCl. The optimum conditions were found to be reaction temperature of 533 K, reaction time of 6 h, and dosages of Na-MMT and LiCl as 12% and 1.2% (wt.% of unsaturated fatty acid), respectively. Under the appropriate levels, the yield of dimer acid was 32.37% in three parallel experiments.

Catalytic synthesis of dimer acids by OMMT. In order to investigate the influence of the interlayer spacing on the yield of dimer acid, Na-MMT was replaced with OMMT, and the optimized reaction conditions from above were used. The results are shown in Table 4, and it can be seen that the yield of dimer acid varied greatly with the interlayer spacing from 33.55% to 70.15%. This could be because the unsaturated fatty acid dimerization occurred in the layered structure of OMMT. A larger layer spacing can provide sufficient reaction space, contribute to the formation of larger volume of dimer acid molecules, and, finally, make it easier for the product to diffuse out of the layered structure.

Reusability of catalysts. The reusability of the catalyst is shown in Figure 9.

As shown in Figure 9, after repeated use of five times the yield decreases slightly ranging from 4.12% to 6.62% for the five second-insert OMMT, and 13.51%~15.90% for the four first-insert OMMT. Therefore, the second-insert OMMT catalysts are the best choice for repeated use. However, the yield of Na-MMT decreased from 32.37% to 9.09%, suggesting a poor performance of its reusability.

Table 4. The interlayer spacing and catalytic properties of OMMT (3 CEC of the first-insert OMMT was used, and 2 CEC of the second-insert OMMT was used).

OMMT	Layer spacing/nm	Yield of dimer acid/%
DTAB-MMT	1.97	33.55
CTAB-MMT	3.80	52.86
HTAC-MMT	3.82	53.40
STAC-MMT	4.06	56.90
DTAB-DTAB-MMT	1.81	43.28
DTAB-CTAB-MMT	3.85	67.32
CTAB-CTAB-MMT	3.82	66.73
HTAC-STAC-MMT	4.01	70.11
STAC-STAC-MMT	4.03	70.15
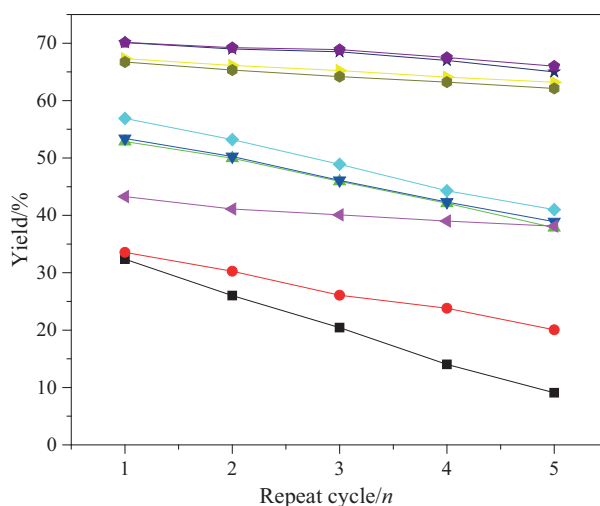
Figure 9. Reusability of Na-MMT and modified OMMT. ⬣STAC-SATA-MMT; ★HTAC-HTAC-MMT; ▶DTAB-CTAB-MMT; ⬠CTAB-CTAB-MMT; ◆STAC-MMT; ▼HTAC-MMT; ▲CTAB-MMT; ◀DTAB-CTAB-MMT; ●DTAB-MMT; ■Na-MMT.

Structural analysis of dimer acid. FT-IR analysis: In the FT-IR spectrum of the dimer acid product shown in Figure 10, there is a wide and strong absorption peak between 3200 and 2500 cm^{-1}, which indicated that the product had a hydroxyl characteristic peak in the form of dimeric polymer. The strong absorption peak at 1710 cm^{-1} was caused by C=O infrared absorption. The peaks at 1377 cm^{-1} and 1460 cm^{-1} were the bending vibrational peaks of methyl (–CH$_3$) and methylene (–CH$_2$) groups, respectively. The stretching vibration peak of –C–O in the carboxyl group appeared at 1285 cm^{-1}, and the peak at 936 cm^{-1} was the surface deformation absorption peak of –OH in the carboxyl group, which indicates that the product was a carboxylic acid. There was no characteristic absorption peak of C=O near 1690~1680 cm^{-1}, indicating that C=O and C=C bonds in the molecule were not conjugated. Furthermore, the characteristic absorption peak of aromatic hydrocarbon near 1600 cm^{-1}, was not observed, indicating that there was a low content of aromatics in the product. The characteristic absorption peak of –(CH$_2$)$_n$– ($n \geq 4$) was found at 723 cm^{-1}, indicating the presence of a straight chain with a large number of –(CH$_2$)$_n$ ($n \geq 4$) structural units. Based on the above information, it is evident that the synthesized products are linear chain dimer acid and single ring dimer acid.

ESI-MS: Mass spectra (Figure 11) of dimer acids were generated by bombardment under negative ion

conditions and so the molecule being analyzed loses a H atom. The relative molecular weight of the dimer acid was 562.9. After losing a H atom, the relative molecular weight of the compound would be around 561.9; therefore the peak at 561.3 corresponds to the dimer acid.
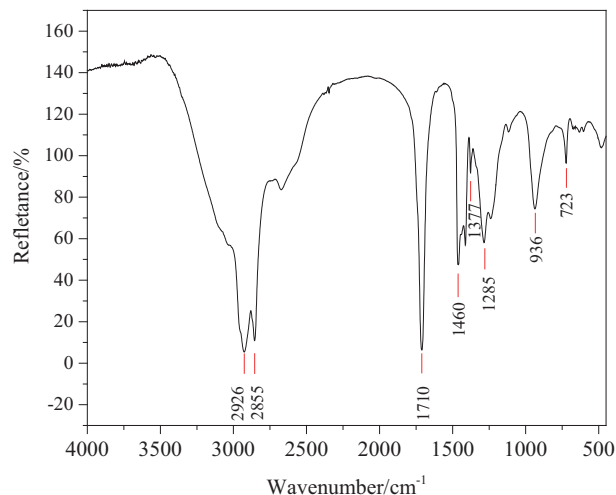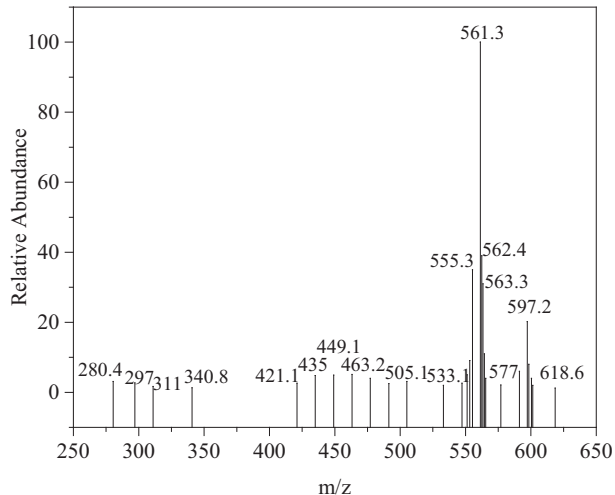

Figure 10. FT-IR spectra of dimer acid.

Figure 11. The mass spectrum of dimer acid.

^{1}H NMR: Figure 12a shows the ^{1}H NMR spectrum of unsaturated fatty acid, the signal at $\delta = 2.79$ ppm corresponds to the characteristic peak of CH=CHC$\underline{\boldsymbol{H}}_2$CH=CH of linoleic acid, while the peaks at $\delta = 5.34$ ppm belong to linoleic acid C$\underline{\boldsymbol{H}}$=C$\underline{\boldsymbol{H}}CH_2C\underline{\boldsymbol{H}}$=C$\underline{\boldsymbol{H}}$ and oleic acid CH$_2$C$\underline{\boldsymbol{H}}$=C$\underline{\boldsymbol{H}}CH_2$. Figure 12b is the ^{1}H NMR spectrum of the dimer acid, product. In Figure 12b, there are no signal peaks at $\delta = 2.79$ ppm and $\delta = 5.31$ ppm, indicating that linoleic acid in the starting material had been completely reacted and oleic acid was also fully involved in the reaction. The peaks at $\delta = 4.80 \sim 5.60$ ppm and $\delta = 6.60 \sim 7.20$ ppm correspond to the hydrogen atoms of the alkene units and the aromatic ring, respectively. The presence of aromatic hydrogen atoms indicated that not only the Diels–Alder reaction occurred in the synthesis of the dimer acid, but also the dehydrogenation of the six membered ring.

Reaction mechanism. The possible reactions of oleic acid and linoleic acid in unsaturated fatty acids are shown in Figure 13.

The carbenium ions mechanism is shown in Figure 13a. MMT acts as Lewis acids generating carbenium ions, and the double bond of the unsaturated fatty acid is protonated under the action of Lewis acid to form carbenium ions and to attack the double bond of another unsaturated fatty acid to produce a linear dimer acid. The Diels–Alder mechanism is shown in Figure 13b; conjugated linoleic acid reacts combining two molecules via electrophilic addition in the double bond position to form a cyclic dimer acid.

3. Conclusions

Cationic surfactants were used to modify the Na-MMT catalyst, and the first- and second-insert OMMT samples were prepared. XRD, SEM, TEM, and FT-IR analyses showed that the structure of the MMT material was maintained and the interlayer spacings increased significantly after the intercalation of the surfactant molecules. The results of dispersion tests showed that the OMMT material became lipophilic after modification of the hydrophilic MMT.

The dimer acid was synthesized under atmospheric pressure, with different MMT samples as catalyst. The catalytic performance of the MMT samples followed the order: OMMT > first-insert OMMT > Na-
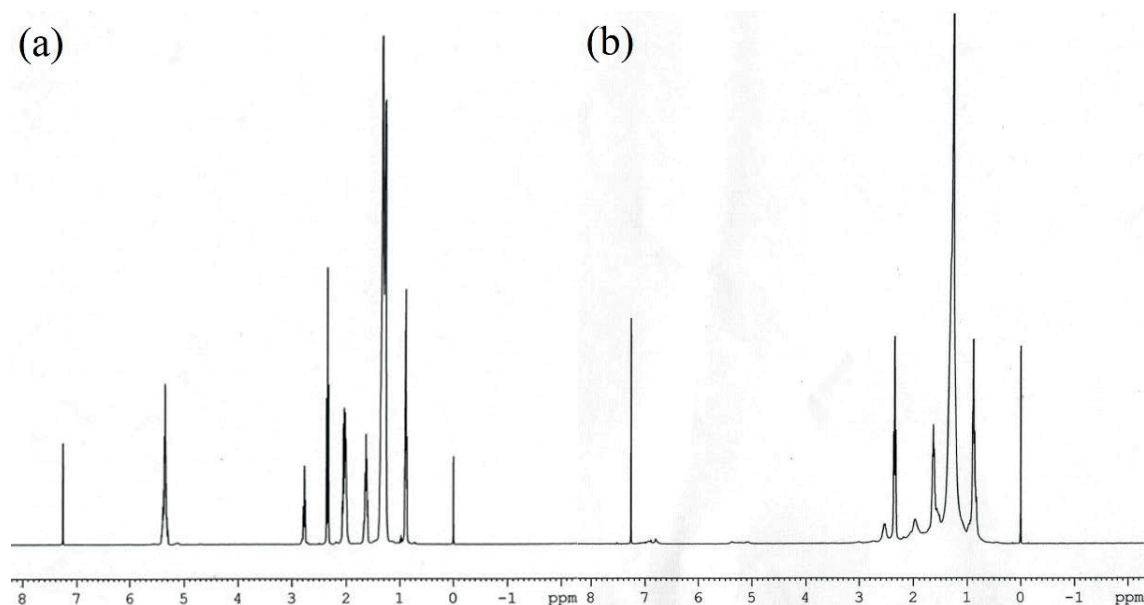
Figure 12. ^{1}H NMR spectra (300 MHz, CDCl$_3$) of (a) unsaturated fatty acid, (b) dimer acid from the polymerization of unsaturated fatty acid at 533 K with OMMT and LiCl for 6 h.
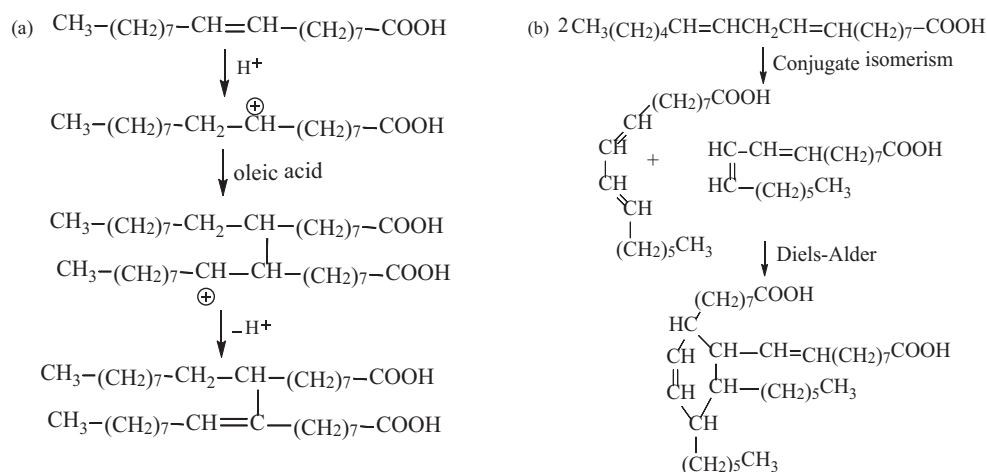

Figure 13. The polymerization mechanism of (a) oleic acid and (b) linoleic acid under the catalytic conditions of OMMT.

MMT. Thus, it is evident that the wider the interlayer spacing, the stronger the dispersion and the better is the catalytic performance. The findings of this work can potentially guide the development of more effective clay-based catalysts for the synthesis of dimer acids.

4. Experimental

4.1. Materials

Na-montmorillonite (Na-MMT) with cation exchange capacity (CEC) value of 90 mmol/100 g was collected from Zhejiang Fenghong clay chemical Co., Ltd. Hexadecyl trimethyl ammonium chloride (HTAC, >99%), stearyl trimethyl ammonium chloride (STAC, >99%) and LiCl (>99%) were purchased from Energy Chemical (China); hexadecyl trimethyl ammonium bromide (CTAB, ≥99%), dodecyl trimethyl ammonium bromide

(DTAB, $\geq 99\%$), and silver nitrate ($\geq 99.8\%$) were purchased from Aladdin Industrial Corporation; unsaturated fatty acid (main fatty acid components: $C_{16:0}$ 1.5%, $C_{18:0}$ 3.9%, $C_{18:1}$ 33.1%, $C_{18:2}$ 59.2%, $C_{18:3}$ 2.3%) was purchased from Liancheng Baixin Science and Technology Co., Ltd. All solvents used were of analytical grade.

4.2. Organic modification of Na-MMT

4.2.1. First-insert OMMT

In a typical preparation of the first-insert OMMT, 10 g of Na-MMT was first added to 300 mL of deionized water and mixed at 500 rpm in a water bath at 348 $\pm$ 1 K for 30 min in order to obtain a high swelling value. DTAB, CTAB, HTAC, and STAC were selected as the intercalation reagents, and they were weighed out such that their mass was 1, 2, and 3 times that of the CEC of Na-MMT. Then the intercalation reagents were added to the Na-MMT suspension under vigorous stirring at 348 $\pm$ 1 K for 3 h. The final mixture was centrifuged and subsequently washed with deionized water until free from halide ion (tested by 0.01 mol/mL $AgNO_3$ solution, until there was no yellow precipitate). The obtained first-insert OMMT (HTAC-MMT, STAC-MMT, DTAB-MMT, and CTAB-MMT) were dried at 363 K for 24 h and pulverized to pass through a 200 mesh sieve.

4.2.2. Second-insert OMMT

After the first intercalation treatment, 10 g of HTAC-MMT (or STAC-MMT, DTAB-MMT, and CTAB-MMT) was added to 300 mL of deionized water and mixed at 500 rpm in a water bath at 333 $\pm$ 1 K for 30 min in order to obtain a high swelling value. The mass of HTAC (or STAC, DTAB, and CTAB) was weighed out to be 1, 2, and 3 times the CEC of Na-MMT, which was then added to the first-insert OMMT suspension under vigorous stirring. The mixture was stirred at 333 $\pm$ 1 K for 3 h. The final mixture was centrifuged and subsequently washed with deionized water until free from halide ion. The obtained second-insert OMMT was dried at 363 K for 24 h and pulverized to pass through a 200 mesh sieve.

4.3. Dispersion test

The dispersion characteristics of OMMT in unsaturated fatty acids were investigated. The OMMT (5 g) was added to 100 mL of the dispersion medium, stirred at high speed for 15 min, kept for 24 h, and then the settling behavior of OMMT was observed.

4.4. Dimer acid synthesis

A three-necked flask was charged with 100 g of unsaturated fatty acid, a certain amount of Na-MMT and LiCl, and then fitted with a condenser tube, thermometer, and agitator. The mixture was stirred under nitrogen atmosphere at ambient pressure and heated at the reaction temperature for the specified reaction time. After completion of the reaction, the crude product was filtered to remove MMT. The content of dimer acid in the crude product was analyzed by HPLC and the yield was calculated.

The as-prepared first-insert and second-insert OMMT catalysts were also used instead of Na-MMT to synthesize the dimer acids.

The yield of dimer acid was calculated in formula (1).

$$the\,yield\,(\%) = \frac{n_1}{n_0} \times 100\% \tag{1}$$

n_1-the molar content of the dimer acid;
n_0-the molar content of unsaturated fatty acid.

4.5. Characterization

The samples were characterized by FT-IR spectra (Spectrum 2000), TG (NETZSCH TG209), XRD (Empyrean diffractometer), SEM views (KYKY-2800B), and TEM (JEM-2010HR). The dimer acids in the product were analyzed by HPLC (Agilent 1200), ^{1}H NMR (Bruker AVANCE AV 400), and LC-MS (TSQ Quantum Ultra).

Acknowledgments

References

1. Leonard, E. C. *J. Am. Oil Chem. Soc.* **1979**, *56*, 782-785.

2. Freitas, R. F. R.; Klein, C.; Pereirac, M. P.; Duczinski, R. B.; Einloft, S.; Seferin, M.; Ligabue, R. *J. Adhes. Sci. Technol.* **2015**, *29*, 1-13.

3. Reulier, M.; Avérous, L. *Eur. Polym. J.* **2015**, *67*, 418-427.

4. Matadia, R.; Hablotb, E.; Wanga, K.; Bahloulia, N.; Ahzia, S.; Avérous, L. *Compos. Sci. Technol.* **2011**, *71*, 674-682.

5. Den Otter, M. J. A. M. *Fett Wiss. Technol.* **1970**, *72*, 1056-1066.

6. Den Otter. M. J. A. M. *Fett Wiss. Technol.* **1970**, *72*, 875-883.

7. Den Otter. M. J. A. M. *Fett Wiss. Technol.* **1970**, *72*, 667-673.

8. Elsasser, F. A.; Mccargar, L. A. US Patent 6187903, 2001-02-08.

9. Unverferth, M.; Meier, M. A. R. *Eur. J. Lipid Sci. Tech.* **2016**, *118*, 1470-1474.

10. Rajiadhyaksha, R. A.; Chaudhari, D. D.; Joshi, G. W. *J. Am. Oil Chem. Soc.* **1988**, *65*, 793-797.

11. Sakai, K.; Saito, Y.; Kitiyanan, B.; Uka, A.; Endo, T.; Matsuda, W.; Sakai, H.; Takamatsu, Y.; Abe, M. *J. Oleo Sci.* **2013**, *62*, 489-498.

12. Číčel, B.; Komadel, P.; Nigrin, M. *Collect. Czech. Chem. C.* **1992**, *57*, 1666-1672.

13. Möhring, H.; Spiteller, G. *Fett Wiss. Technol.* **1990**, *92*, 126-131.

14. Nascimento, A. R. d.; Alves, J. A. B. L. R.; Melo, M. A. d. F.; Melo, D. M. d. A. *J. Mater. Res.* **2015**, *18*, 283-287.

15. McMahon, D. H.; Crowell, E. P. *J. Am. Oil Chem. Soc.* **1974**, *6*, 522-527.

16. Picard, E.; Espuche, E.; Fulchiron, R. *Appl. Clay Sci.* **2011**, *53*, 58-65.

17. González, A.; Dasari, A.; Herrero, B.; Plancher, E.; Santarén, J.; Esteban, A.; Lim, S. H. *Polym. Degrad. Stabil.* **2012**, *97*, 248-256.

18. Hojiyev, R.; Ersever, G.; Karaağaçlıoğlu, I. E.; Karakaş, F.; Boylu, F. *Appl. Clay Sci.* **2016**, *127-128*, 105-110.

19. Komadel, P.; Madejová, J.; Bujdák, J. *Clay Clay Miner.* **2005**, *53*, 313-334.

20. Komadel, P.; Schmidt, D.; Madejová, J.; Číčel, B. *Appl. Clay Sci.* **1990**, *5*, 113-122.

21. Hinze, D. A. G. *Fette Seifen Anstr.* **1986**, *88*, 530-533.

22. Izumi, Y.; Urabe, K.; Onaka, M. *Catal. Surv. Asia.* **1997**, *21*, 227-233.

23. Lide, D. R. *CRC Handbook of Chemistry and Physics;* 88th Eds. CRC Press: Boca Raton, FL, USA, 2007.

24. Wu, D.; Wu, L.; Wu, L.; Zhang, M. *Polym. Degrad. Stabil.* **2006**, *91*, 3149-3155.

25. Bourbigot, S.; Fontaine, G.; Bellayer, S.; Delobel, R. *Polym. Test.* **2008**, *27*, 2-10.

26. Zhou, L. M.; Chen, H.; Jiang, X. H.; Lu, F.; Zhou, Y. F.; Yin, W. M.; Ji, X. Y. *J. Colloid Interf. Sci.* **2009**, *332*, 16-21.